TISSUE ENGINEERING: Part A
Volume 18, Numbers 7 and 8, 2012

DOI: 10.1089/ten.tea.2011.0391

Improving Viability of Stem Cells During Syringe Needle Flow Through the Design of Hydrogel Cell Carriers

Brian A. Aguado, B.S.,[1] Widya Mulyasasmita, M.S.,[1] James Su, Ph.D.,[2]
Kyle J. Lampe, Ph.D.,[2] and Sarah C. Heilshorn, Ph.D.[2]

Cell transplantation is a promising therapy for a myriad of debilitating diseases; however, current delivery protocols using direct injection result in poor cell viability. We demonstrate that during the actual cell injection process, mechanical membrane disruption results in significant acute loss of viability at clinically relevant injection rates. As a strategy to protect cells from these damaging forces, we hypothesize that cell encapsulation within hydrogels of specific mechanical properties will significantly improve viability. We use a controlled *in vitro* model of cell injection to demonstrate success of this acute protection strategy for a wide range of cell types including human umbilical vein endothelial cells (HUVEC), human adipose stem cells, rat mesenchymal stem cells, and mouse neural progenitor cells. Specifically, alginate hydrogels with plateau storage moduli (G') ranging from 0.33 to 58.1 Pa were studied. A compliant crosslinked alginate hydrogel ($G' = 29.6$ Pa) yielded the highest HUVEC viability, 88.9% ± 5.0%, while Newtonian solutions (i.e., buffer only) resulted in 58.7% ± 8.1% viability. Either increasing or decreasing the hydrogel storage modulus reduced this protective effect. Further, cells within noncrosslinked alginate solutions had viabilities lower than media alone, demonstrating that the protective effects are specifically a result of mechanical gelation and not the biochemistry of alginate. Experimental and theoretical data suggest that extensional flow at the entrance of the syringe needle is the main cause of acute cell death. These results provide mechanistic insight into the role of mechanical forces during cell delivery and support the use of protective hydrogels in future clinical stem cell injection studies.

Introduction

Direct injection is often the clinically preferred method of cell transplantation due to its minimally invasive nature.[1–5] Cell injection therapies have shown immense potential in improving tissue and organ function for multiple debilitating diseases and injuries including peripheral arterial disease,[6] myocardial infarct,[7–10] stroke,[11–13] Parkinson's disease,[14] and paralysis.[15] Unfortunately, several obstacles prevent these cell transplantation procedures from being translated to the mainstream clinical environment. Increasing the percentage of live cells post-injection is critical to the success of the cell transplantation procedure.[16] Previous studies have correlated symptomatic relief with higher cell viability after transplantation.[1,17,18] Cell injection procedures typically result in a deficit of live cells, with viabilities as low as 1%–32% post-transplantation.[19]

Many cell injection studies have focused on the role of the host microenvironment as a contributing factor to low transplanted cell viability.[20–22] For example, upon injection into ischemic tissue for therapeutic repair, cells experience a harsh hypoxic microenvironment and an acute immune response, both of which are thought to negatively impact cell viability.[23] Regardless of the detrimental host microenvironment, the first point of cell damage may occur during the actual injection procedure. The mechanical disruption of cells during the injection process is not commonly recognized as a source of cell death. We suggest that injected cell viability could be improved by providing an injectable scaffold that protects cells from the damaging injection process. Further, design of injection protocols currently relies on trial-and-error empirical studies and the surgeon's personal experience.[24] To increase the efficiency of stem cell transplantations, delivery modalities must be improved to accelerate the translation of these therapies to the clinic.

Hydrogels as cell carriers have shown potential to improve current transplantation techniques.[14] For example, cell injections using Matrigel, a complex hydrogel mainly composed of laminin, as a cell carrier demonstrated improved transplanted cell outcomes.[21,25] However, Matrigel is derived from mouse sarcoma cells and is not preferred for clinical applications in humans. Much of the recent research on hydrogel cell carriers has focused on the role of these materials post-delivery to the target tissue or organ. For

Departments of [1]Bioengineering and [2]Materials Science and Engineering, Stanford University, Stanford, California.

example, hydrogels may act as scaffolds for local cell adhesion,[7,21] allowing for additional control over implant localization at the target site and for support of new tissue growth.[10,22,26] Additionally, hydrogels may be designed to protect encapsulated cells from local inflammation and surrounding macrophages.[27] Certain hydrogels may also strategically deliver anti-apoptotic or pro-stimulatory factors.[1] In contrast, here we focus on the role of hydrogels during the injection procedure (as opposed to post-delivery), when the presence of a viscoelastic material may serve to protect cells from the damaging mechanical forces experienced during flow.

We have chosen alginate as a model hydrogel to determine the impact of cell carrier mechanics on cell viability during ejection from a syringe needle. Alginate, an inexpensive and biocompatible biopolymer, is composed of long chains of individual sugar residues β-D-mannuronate (M-subunits) and α-L-guluronate (G-subunits).[28–30] During crosslinking, one calcium ion coordinates with four G-subunits to form a hydrogel network. The resulting hydrogel mechanics can be tailored by altering the degree of crosslinking, making it attractive for tissue engineering and cell delivery applications.[29,31] Further, alginate can be shear thinned and is therefore a promising material for cell delivery applications involving injection through a needle or catheter.[31–33] Alginate has been utilized in preclinical injection studies to provide a temporary cellular scaffold and to attenuate adverse cardiac remodeling.[32,34] After shear thinning, alginate is able to regain its original crosslinked structure, resulting in a bulk hydrogel that supports cell growth at the transplant site.[35] The successful use of alginate in a variety of preclinical tissue engineering and injection protocols supports the further study of this material as a potential cell-carrying hydrogel for clinical use.

Here, we elucidate the mechanical mechanisms that negatively affect acute cell viability during syringe needle flow and demonstrate a simple hydrogel strategy to overcome these limitations. By systematically comparing the effects of shear stress with extensional flow (which is experienced during syringe needle ejection) to the effects of shear stress alone, we identified extensional flow as a major cause of acute cell death. We further demonstrated that cells are protected from the damaging effects of extensional flow by pre-encapsulating them within alginate hydrogels of intermediate stiffness ($G' \sim 30$ Pa). These results support the investigation of hydrogel materials with optimized viscoelastic properties in preclinical and clinical cell transplantation studies to potentially mitigate the damaging effects of extensional flow.

Materials and Methods

Alginate formulation and preparation

Ultra-pure alginate (75, 147, and 200 kDa; NovaMatrix, Sandvika, Norway) solutions were prepared on ice using a digital sonicator and sterilized via syringe filtration (2% wt/vol in phosphate-buffered saline [PBS], pH 7.4). Hydrogels (1% wt/vol final concentration) were prepared by mixing equal volumes of alginate and calcium chloride (Sigma-Aldrich, St. Louis, MO) solutions to achieve a final stoichiometric ratio of 0.5:4 or 1:4 (Ca^{2+} ion:G-subunit).

Rheology of alginate solutions and hydrogels

Dynamic oscillatory rheology. Experiments were performed on an MCR301 rheometer at 25°C with a humidity chamber (Anton Paar, Ashland, VA). Noncrosslinked alginate samples (1% wt/vol in PBS) were characterized using conical plate geometry (50 mm diameter, 1° cone angle) with frequency sweeps from 0.1 to 100 s^{-1} and shear strain of 5% ($n = 3$). Crosslinked alginate samples ($n = 3$) were characterized using parallel plate geometry (25 mm diameter, 1 mm gap height), frequency sweeps of 0.1 to 100 s^{-1}, and shear strain of 5%.

Linear shear rheology. Experiments were performed on an ARG2 rheometer (TA Instruments, New Castle, DE) with conical plate geometry (20 mm diameter, 1° cone angle). Solutions were directly prepared on the platform, and a linear shear rate sweep from 10 to 10,000 s^{-1} was applied. Shear-thinning experiments were performed by applying a constant linear shear rate of 5.3 s^{-1} for 100 s (which matches the shear rate inside the syringe barrel), then applying a constant high shear rate of 17,240 s^{-1} for 300 s (which is the same order of magnitude as the maximum shear rate predicted to occur in a 28-gauge syringe needle and the maximum shear rate possible on the ARG2 rheometer), and finally allowing the hydrogel to recover by applying a shear rate of 5.3 s^{-1} for 100 s.

Pressure measurements during syringe needle flow

All samples (50 μL each) were loaded into 28-gauge, 1-mL syringes (diameter = 3.17 mm; BD Biosciences, Franklin Lakes, NJ) mounted on a syringe pump (SP220I; World Precision Instruments, Sarasota, FL). A compression load cell (LCKD-500; Omegadyne, Sunbury, OH) was fitted in direct contact between the pump pusher block and the syringe plunger. A digital panel meter (DP41-S; Omegadyne) displayed the measured force during ejection at a constant flow rate of 1000 μL/min ($n = 5$). The peak force divided by the syringe cross-sectional area gives the ejection pressure, and the pressure drop is defined as the difference between the entrance pressure applied at the plunger and the exit pressure at the needle opening.[31]

Cell culture

Human umbilical vein endothelial cells (HUVEC) were cultured on tissue culture polystyrene (TCPS) dishes (BD Biosciences) using EBM-2 HUVEC growth medium containing 10% fetal bovine serum (FBS; Lonza, Basel, Switzerland). Human adipose stem cells (hASC) were cultured in 1× Dulbecco's Modified Eagle Medium (Invitrogen, Carlsbad, CA) containing 15% FBS and 1.5% penicillin-streptomycin solution on Primeria culture dishes (BD Biosciences). Both hASC and HUVEC were used within passages 3–8. Rat mesenchymal stem cells (rMSC) were cultured on TCPS dishes using rat marrow stem cell growth medium (Cell Applications, San Diego, CA) with 10% FBS. Cultures of rMSC from passage 40 were used. HUVEC, hASC, and rMSC were passaged using TrypLE Express (Invitrogen). Primary mouse neural progenitor cells (mNPC) isolated from the adult murine dentate gyrus were cultured in Neurobasal A medium (Invitrogen) containing 20 ng/mL epidermal growth factor (Peprotech, Rocky Hill, NJ), 20 ng/mL fibroblast growth factor (Peprotech),

1% Glutamax (Invitrogen), and 2% B27 media supplement (Invitrogen). mNPC were expanded on polyornithine (0.67 μg/cm^2) and laminin (0.33 μg/cm^2) coated TCPS. mNPC were passaged using 0.025% trypsin/EDTA, and passages 10–11 were used for experiments. All cells were cultured in a humidified 5% CO_2 incubator at 37°C. Initial cell viability was quantified using Trypan Blue (Invitrogen).

Cell encapsulation and syringe needle flow viability assay

Cells were resuspended at a cell density of 4.0×10^4 cells/μL in either PBS or calcium-enhanced media (prepared from stock of 1% $CaCl_2$ dissolved in culture media, diluted with sterile PBS to achieve a final Ca^{2+} ion to G-subunit ratio of 0.5:4 or 1:4). The cell suspension (25 μL) was mixed with an equal amount of 2% wt/vol alginate solution, loaded into a 1-mL syringe with 28-gauge needle, mounted onto the syringe pump, and ejected onto a sterile glass coverslip at a constant volumetric flow rate of 1000 μL/min. Cell viability was assessed with a LIVE/DEAD assay (Invitrogen) by incubating at 37°C for 45 min with 2 μM calcein-AM and 4 μM ethidium homodimer-1 in PBS. Nonejected samples were controls during all trials. Samples were imaged using a Zeiss Axiovert 200M fluorescence microscope and quantified using ImageJ software (NIH freeware). Between 4 and 25 independent trials were conducted for each cell carrier formulation (see Table 1). The sample mean viability was calculated and normalized to the initial viability of the culture. Statistical significance was determined using the Student's *t*-test with $p < 0.05$. Error bars on all figures represent the standard deviation of the sample mean.

Linear shearing of encapsulated HUVEC

Given conservation of mass, the linear fluid velocity within the needle, v, is determined using: $v = Q/\pi r^2$; where Q is the volumetric flow rate (1000 μL/min) and r is the internal radius of the needle (0.0925 mm). The shear rate at the wall of a pipe for a Newtonian fluid, γ', is given by the equation: $\gamma' = 4v/r$; yielding a linear shear rate of 26,800 s^{-1}. HUVEC were suspended in PBS, a 1% wt/vol noncrosslinked alginate solution (MW = 75 kDa), or a 1% wt/vol 1:4 crosslinked alginate hydrogel (MW = 75 kDa). Linear shear of 17,240 s^{-1} was applied to the cell mixtures for 5 s using a conical plate rheometer. Nonsheared samples acted as controls. Cell viability was evaluated using the LIVE/DEAD assay as above.

Finite element simulation of syringe needle flow

Fluid flow simulation was conducted in Comsol 4.0a (Comsol, Palo Alto, CA) using a mesh of free tetrahedral elements and boundary conditions of 1000 μL/min at the inlet and atmospheric pressure at the outlet. An incompressible, Newtonian fluid model was used to simulate the flow of PBS at 20°C, with a constant density of 998.2 kg/m^3 and viscosity of 1.005 cP. A non-Newtonian fluid model was used to simulate the flow of noncrosslinked alginate using a power-law, shear-rate dependent relationship.[31] An incompressible fluid of alginate solution (MW = 200 kDa) was assumed to have a constant density of 1016 kg/m^3, and empirically obtained constants n and K of 0.7852 and 0.1078, respectively. See Supplementary Data (Supplementary Fig. S1 and Supplementary Table S1; Supplementary Data are available online at www.liebertonline.com/tea) for rheology fitting data to determine n and K. All simulations were found to be grid-independent and convergence criterion independent after extra fine, fine, and normal mesh settings were studied, and all discretization errors converged to zero.

Results

Crosslinked alginate is cell protective during syringe needle flow

In the absence of calcium, alginate solutions freely flow as viscous liquids. The addition of Ca^{2+} ions to an alginate

Table 1. Compositions and Properties of Various Cell Carriers

	Cell carrier[a]	*Ca^{2+}: G-subunit*	*η [cP]*[b]	*Plateau G′ [Pa]*	*Pressure drop [kPa]*[c]	*Sample size (n)*[d]
Newtonian fluid	PBS	–	1.005	–	178.65 ± 12.16	25
	Glycerol (% wt/vol)					
	10	–	7.53 ± 0.41	–	169.78 ± 37.25	6
	35	–	9.19 ± 0.19	–	198.93 ± 15.20	18
	40	–	10.34 ± 0.44	–	203.99 ± 41.12	18
Viscoelastic fluid	1% wt/vol Alginate (kDa)					
	75	0	9.30 ± 0.14	–	191.32 ± 12.62	10
	147	0	18.39 ± 0.46	–	197.66 ± 17.81	4
	200	0	20.64 ± 1.39	–	259.74 ± 49.59	10
Viscoelastic gel	75	0.5:4	9.51 ± 0.02	0.33 ± 0.22	215.40 ± 24.35	6
	147	0.5:4	18.48 ± 0.20	0.58 ± 0.31	305.36 ± 36.41	6
	200	0.5:4	19.83 ± 0.81	2.96 ± 2.19	406.72 ± 19.66	6
	75	1:4	11.82 ± 1.03	29.57 ± 0.99	292.69 ± 15.43	15
	147	1:4	24.90 ± 0.80	47.02 ± 2.42	405.45 ± 35.64	12
	200	1:4	32.17 ± 0.37	58.14 ± 4.55	642.39 ± 49.93	12

[a]All solutes were dissolved in PBS.
[b]Viscosity values were obtained at shear rate of 17,240 s^{-1}.
[c]Sample size for pressure drops was $n = 5$ for each experiment.
[d]Sample size was specific to HUVEC ejection experiments.
HUVEC, human umbilical vein endothelial cells; PBS, phosphate-buffered saline.

solution forms a highly crosslinked alginate hydrogel which holds its shape (Fig. 1A). When HUVEC were subjected to syringe needle flow within a PBS cell carrier at a flow rate of 1000 μL/min, the acute cell viability was observed to be only 58.7%±8.1% (Fig. 1B). Suspending HUVEC within crosslinked alginate (1% wt/vol, 1:4 crosslinking ratio) significantly improved acute viability of ejected cells to 88.9%±5.0%, 74.7%±4.5%, and 72.1%±7.8% for the 75, 147, and 200 kDa hydrogels, respectively ($p<0.05$). In contrast, noncrosslinked alginate (i.e., a nongelled, viscous alginate solution) did not provide any cell protection, resulting in acute viability of 66.9%±11.0%, 54.2%±11.1%, and 59.4%±13.7%, for the 75, 147, and 200 kDa solutions, respectively. As positive controls, nonejected samples of HUVEC within PBS, the 200 kDa alginate hydrogel, or the 200 kDa alginate solution all retained greater than 93% viability. The ability to protect HUVEC from syringe needle flow was found to vary among hydrogels of different polymer molecular weights. Cells encapsulated within the lowest molecular weight 75 kDa hydrogel showed significantly higher viability compared with the 147 and 200 kDa crosslinked gels ($p<0.05$).

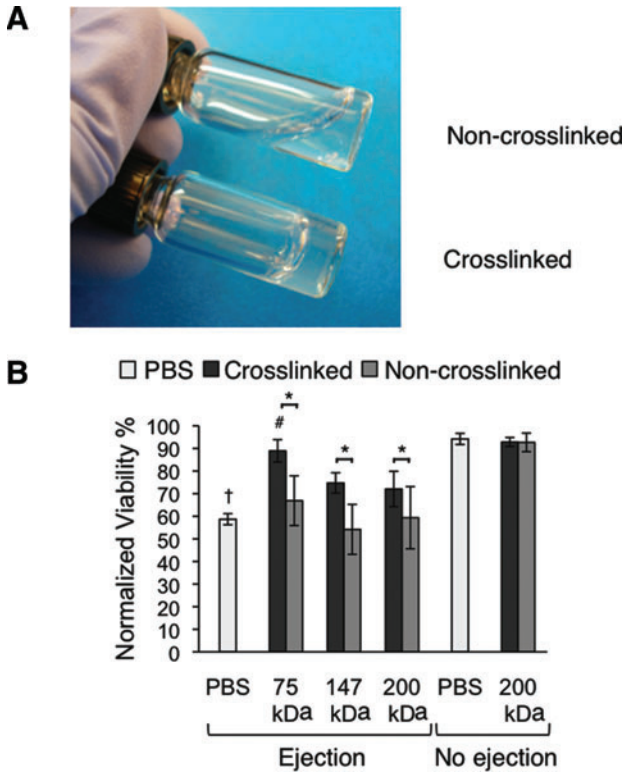

FIG. 1. Cell viability after syringe needle flow. **(A)** Photograph of 1% wt/vol, 200 kDa alginate without (top) and with (bottom) crosslinking (1:4 Ca^{2+} ion:G-subunit). **(B)** HUVEC viability within PBS, 1:4 crosslinked alginate gels, or noncrosslinked alginate solutions with and without ejection through a syringe needle, *$p<0.05$. † indicates statistical significance between PBS and all ejected crosslinked alginate gels ($p<0.05$). # indicates statistical significance between ejected 75 kDa crosslinked alginate compared with ejected 147 and 200 kDa crosslinked alginate. HUVEC, human umbilical vein endothelial cells; PBS, phosphate-buffered saline. Color images available online at www.liebertonline.com/tea

Linear shear flow does not cause significant membrane damage

During flow through a syringe needle, the volumetric flow rate (1000 μL/min) is constant through the constriction point between the syringe and needle ($d_{syringe}/d_{needle} \sim 17$). The linear fluid velocities inside the syringe and needle were calculated to be $v_1 = 2.11$ mm/s and $v_2 = 620$ mm/s, respectively (Fig. 2A). Therefore, the linear fluid velocity in the needle is 294× greater than that in the syringe. These linear velocities correspond to shear rates of $5.3\,s^{-1}$ in the syringe and $26{,}800\,s^{-1}$ in the needle. These experimental parameters were used to predict the distribution of shear stress within the syringe and needle using a finite element model (Fig. 2A). Simulations modeling a PBS cell carrier and a noncrosslinked alginate cel carrier were compared. In both cases, the areas of highest shear were found at the needle walls, while the lowest shear was experienced in the syringe. Comparing the two cases, the viscous alginate solution resulted in shear stresses that were ~10× greater than PBS.

To experimentally test the effects of linear shear flow on acute cell viability, a rheometer was utilized to apply a shear rate of $17{,}240\,s^{-1}$ for 5 s. The actual flow time for cells to pass through the 12.7-mm long needle is estimated to be only ~0.02 s (length/v_2 = [12.7 mm]/[620 mm/s]). Within a PBS cell carrier, a noncrosslinked alginate solution, and the crosslinked alginate hydrogel (MW = 75 kDa), the acute viabilities for sheared and nonsheared HUVEC were statistically similar (Fig. 2B).

The mechanical properties of alginate hydrogels can be predictably tailored

Using oscillatory shear rheometry, crosslinked alginate samples demonstrated higher storage moduli (G') than loss moduli (G''), indicating that the materials were indeed hydrogels (Fig. 3A, B). As expected, increasing the molecular weight of the polymer (while keeping crosslinking stoichiometry and polymer concentration constant) resulted in an increase in G' and G''. This trend was exemplified within two families of hydrogels with crosslinking ratios of 1:4 (Fig. 3A) and 0.5:4 (Fig. 3B). The plateau G' within the angular frequency range of 1 to $10\,s^{-1}$ were reported in Table 1 for the six alginate hydrogel formulations. For the noncrosslinked alginate solutions, G'' was shown to be greater than G' for each molecular weight tested, indicating that the materials are viscous solutions and not gels (Fig. 3C). Viscosity measurements at $17{,}240\,s^{-1}$ shear rate were reported in Table 1 for all six alginate hydrogel formulations and three alginate solutions in addition to glycerol control solutions. For both noncrosslinked alginate solutions and crosslinked alginate hydrogels, the viscosity increased with higher molecular weight. As expected, hydrogels with a greater extent of calcium crosslinking had increased viscosity.

Shear rheometry was also utilized to determine the shear-thinning and regelation behavior of the alginate hydrogels under simulated cell transplantation injection protocols. For the stiffest hydrogel tested ($G' = 58.1$ Pa), the linear viscosity remained constant at around 6000 cP at a shear rate of $5.3\,s^{-1}$, similar to the shear experienced within a 1-mL syringe at a flow rate of 1000 μL/min. At a shear rate of $17{,}240\,s^{-1}$, which mimics the flow through a 28-gauge needle at a flow rate of 1000 μL/min, the viscosity dropped to 32.17 cP. Once the

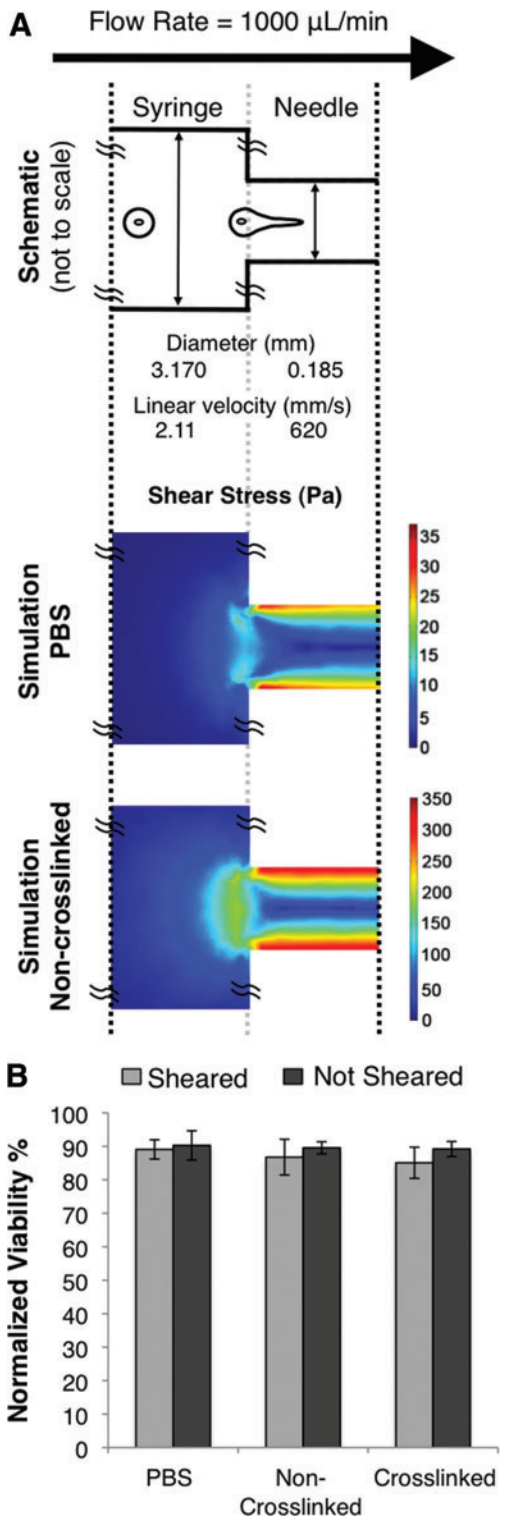

FIG. 2. Flow characteristics during syringe needle flow. **(A)** (Top) Schematic of syringe device, not drawn to scale. (Middle and bottom) Heat map of shear stress during syringe needle flow as obtained by finite element modeling of PBS (middle) and noncrosslinked alginate (bottom). **(B)** HUVEC viability within PBS, noncrosslinked (75 kDa), or crosslinked (75 kDa, 1:4 crosslinking) alginate exposed to a shear rate of 17,240 S^{-1} for 5 s. Color images available online at www.liebertonline.com/tea

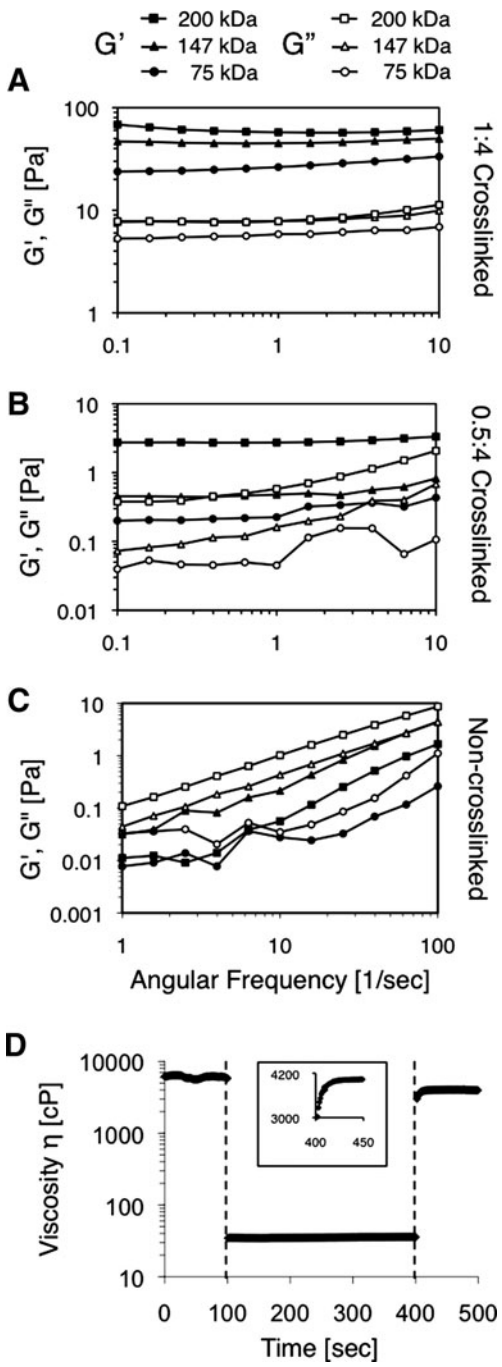

FIG. 3. Rheology of alginate hydrogels and solutions. Storage (G') and loss (G'') moduli of **(A)** 1:4 and **(B)** 0.5:4 crosslinked alginate hydrogels and **(C)** noncrosslinked alginate solutions of varying molecular weight. **(D)** Shear-thinning and recovery behavior of 1:4 crosslinked alginate hydrogel (200 kDa); inset of recovery period.

shear rate was reduced to 5.3 s^{-1}, the viscosity recovered to 4000 cP within 6 s, demonstrating regelation (Fig. 3D).

To characterize the force required to initiate flow, we used a pressure transducer mounted on the syringe pump (Table 1). For Newtonian solutions, larger pressure drops were required for more viscous solutions. As expected, a similar trend was observed for the noncrosslinked alginate solutions; higher molecular weight polymers led to increased

viscosity and greater pressure drops. Similarly, for crosslinked hydrogels, the pressure drop required to drive the flow through the syringe needle increased with larger molecular weight and greater degree of ionic crosslinking.

Cell carrier mechanics impacts viability during syringe needle flow

To determine the effects of various rheological profiles on acute cell protection, we systematically tested cell carriers with three different types of rheological properties in our *in vitro* model of cell injection: Newtonian fluids, viscoelastic fluids, and viscoelastic hydrogels. For all Newtonian fluids (PBS and glycerol solutions), HUVEC viability was significantly decreased in all of the samples exposed to syringe needle flow compared with nonejected samples of the same formulation ($p<0.05$ for all paired comparisons, Fig. 4A). Similarly, for all viscoelastic fluids (noncrosslinked alginate solutions), HUVEC viability was significantly decreased in all of the ejected samples ($p<0.05$, Fig. 1B). For all of these fluid-like cell carriers, the viability of cells exposed to syringe needle flow were statistically similar to that of cells in PBS alone.

In contrast, all six of the crosslinked alginate hydrogels described in Table 1 (with G' values ranging from 0.33 to 58.1 Pa) resulted in ejected cell viabilities that were statistically greater than that of PBS ($p<0.05$, Fig. 4B). As a positive control, nonejected HUVEC encapsulated within the cell carriers maintained a high viability across all G' values. The highest ejected HUVEC viability (88.9%±4.9%) was observed with the hydrogel formulation of $G'=29.6$ Pa. This viability was statistically identical to the positive control of cells dispersed in PBS without exposure to syringe needle flow (94.2%±2.4%). Hydrogels with G' values higher or lower than 29.6 Pa (i.e., stiffer or more compliant gels, respectively) resulted in significantly lower cell viability following syringe needle flow ($p<0.05$ for all comparisons).

Multiple cell types are protected from syringe needle flow by crosslinked alginate

Due to the success of crosslinked alginate in maintaining HUVEC viability during syringe needle flow, these hydrogels were used to provide flow protection for several stem and progenitor cell types: hASC, rMSC, and mNPC ($n=3$ to 10 independent trials). In the absence of syringe needle flow, all three stem cell types maintained statistically similar viabilities whether they were encapsulated within alginate hydrogels or dispersed in PBS. Similar to the previous results with HUVEC, all of the stem cell samples experienced a significant decrease in cell viability during syringe needle flow when delivered in PBS alone ($p<0.05$, Fig. 5A, B). Also similar to the HUVEC results, the alginate hydrogel with $G'=29.6$ Pa was able to provide protection during syringe needle flow for all three stem cell types, resulting in significantly greater cell viability than cells ejected in either PBS or the stiffer alginate hydrogel with $G'=58.1$ Pa ($p<0.05$). All cell types tested displayed a spherical, symmetric morphology as expected for cells held in PBS suspension or encapsulated within alginate hydrogels for less than one hour.

Discussion

Our results demonstrate the protective effects of alginate shear-thinning hydrogels on cells experiencing clinically relevant syringe needle flow. During syringe needle flow, cells experience three types of mechanical forces that can lead to cell disruption: (i) a pressure drop across the cell, (ii) shearing forces due to linear shear flow, and (iii) stretching forces due to extensional flow. In our experimental design, we specifically assay for physical disruption of the cell membrane using ethidium homodimer-1, which is a high-affinity nucleic acid stain that cannot diffuse across an intact lipid bilayer, thereby allowing direct quantification of cells that experience cell membrane damage in response to these mechanical forces.

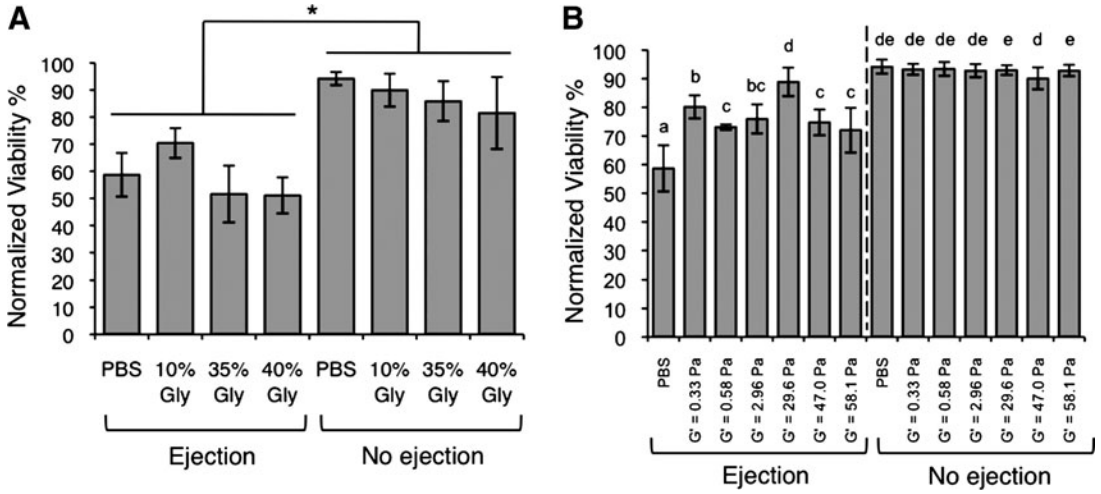

FIG. 4. HUVEC viability after syringe needle flow in various cell carriers. **(A)** Viability within Newtonian fluids (PBS and glycerol solutions) with and without ejection through a syringe needle, $*p<0.05$. **(B)** Viability within PBS and crosslinked alginate hydrogels of varying G' with and without ejection. Statistical significance is represented by letters above each column, with different letters signifying distinct statistical groups, $p<0.05$.

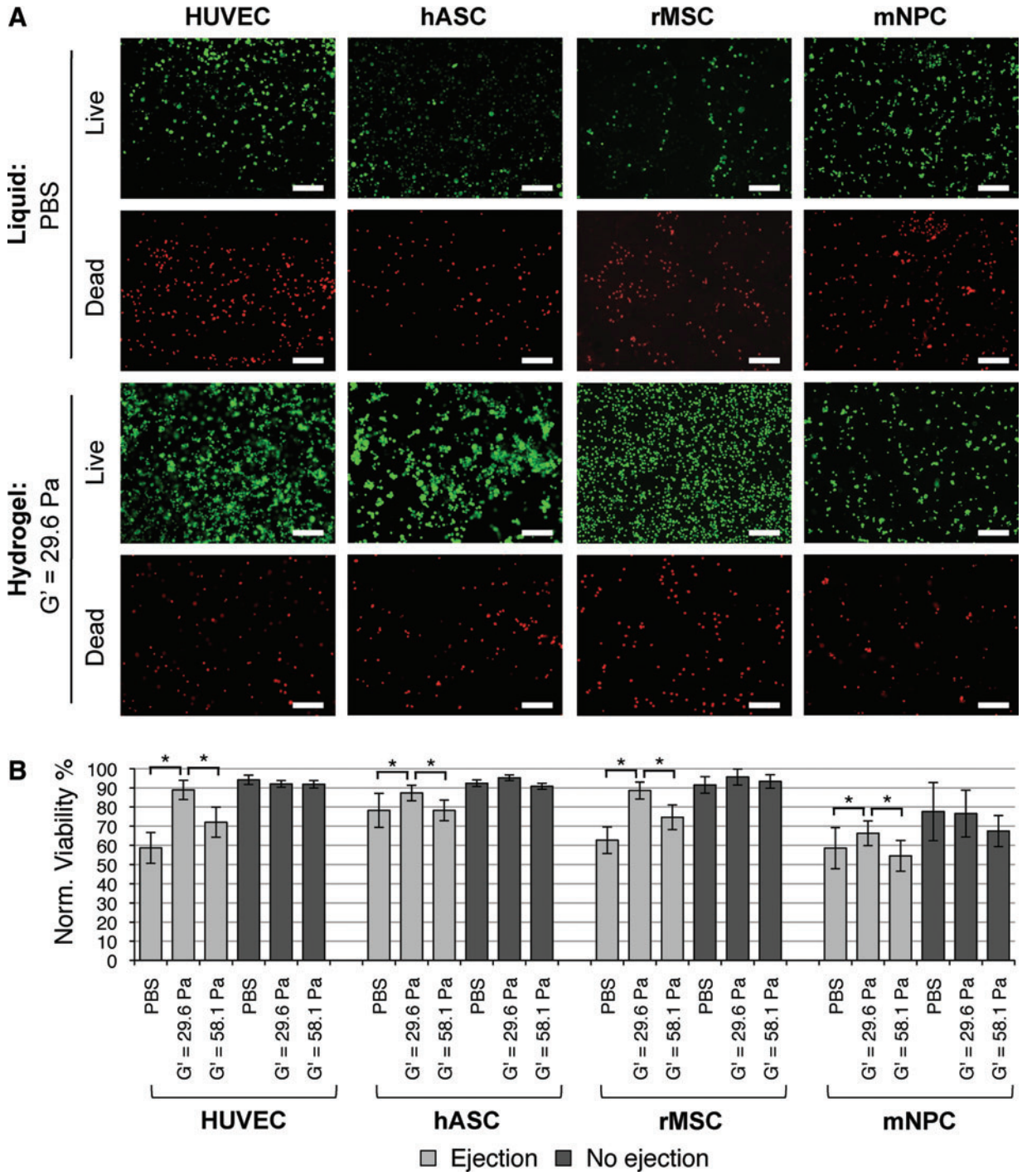

FIG. 5. Viability of HUVEC, hASC, rMSC, and mNPC after syringe needle flow in various cell carriers. **(A)** Fluorescent images of viable (green, calcein AM) and membrane damaged (red, ethidium homodimer-1) cells postejection in PBS or crosslinked alginate hydrogel ($G' = 29.6$ Pa), scale bars = 200 μm. **(B)** Percent cell viability with and without ejection in PBS or alginate hydrogels of $G' = 29.6$ or 58.1 Pa, $^*p < 0.05$. hASC, human adipose stem cells; rMSC, rat mesenchymal stem cells; mNPC, mouse neural progenitor cells. Color images available online at www.liebertonline.com/tea

Extensional flow during ejection is likely the leading cause of acute cell death during syringe needle flow. Pressure drop is not the main cause because we observed that pressure drop did not correlate with cell death in our studies (Table 1, Fig. 4B). In our flow experiments, peak pressure drop for the most protective alginate gel formulation ($G' = 29.6$ Pa) was 292.69 kPa (2.9269 bars, Table 1), while a more compliant alginate gel formulation ($G' = 0.33$ Pa) resulted in a lower peak pressure drop of 215.40 kPa (2.1540 bars, Table 1) but significantly fewer viable cells (Fig. 4B). The pressures measured in our most protective alginate hydrogel (~3 bars) are similar in scale to those previously reported to be

well tolerated in studies of hydrocyclone cell separation protocols.[36]

We next considered the role of shear forces in inducing mechanical disruption of the cell membrane. The maximum shear rate during syringe needle flow occurs at the wall of the needle and was calculated to be 26,800 s^{-1}. A linear shear rate of similar magnitude (17,240 s^{-1}, the maximum rate experimentally possible) was directly applied to cells within a PBS cell carrier using a rheometer. Acute viabilities for both linearly sheared and not sheared cells were greater than 90% and were statistically similar (Fig. 2B); therefore, shearing alone does not significantly disrupt the cell membrane. Taken together, we conclude that the pressure drop and linear shear flow are not the main causes of acute cell death during syringe needle flow.

Extensional flow occurs when there is an abrupt change in the flow geometry causing a dramatic increase in linear velocity. The change in cross-sectional diameter from 3.170 to 0.185 mm as the fluid transitions from the syringe to the needle results in a 294-fold increase in linear velocity (Fig. 2A). Previous experiments have shown that cells undergo significant stretching and deformation in extensional flows, leading to cell death.[37,38] Further, extensional flow is commonly used to stretch and fragment DNA for high throughput sequencing.[39,40] HUVEC in a saline carrier subjected to syringe needle flow (which includes extensional and linear shear flows) resulted in 58.7% viability (Fig. 1B) while cells subjected to linear shear flow alone resulted in 89.1% viability (Fig. 2B). This suggests the leading contributor to acute cell death during syringe needle flow is mechanical disruption caused by extensional flow.

We hypothesized that cell encapsulation within hydrogel cell carriers may provide mechanical protection that prevents the damage caused by extensional flow during injection procedures. To systematically test this hypothesis, we designed a range of alginate hydrogels with varying viscoelastic properties and assessed their protective capabilities. We identified a specific alginate hydrogel formulation ($G' \sim 30$ Pa) that significantly improved the acute cell viability of four different cell types (Figs. 1, 4, and 5). In comparison, noncrosslinked alginate solutions were not cell protective and resulted in low cell viability comparable to PBS-only cell carriers (Fig. 1). Therefore, cell protection is a result of the mechanical properties of the alginate hydrogel and not the biochemical properties of the alginate biopolymers.

Upon ejection, our alginate hydrogels may be experiencing "shear banding" along the inner wall of the needle. During shear banding, a layer of hydrogel near the walls undergoes shear thinning to form a fluid while the rest of the hydrogel remains intact. This layer of shear-thinned fluid acts as a lubricant, allowing the rest of the intact hydrogel to slip through the needle in a process known as "plug flow". Many noncovalently crosslinked hydrogels have been reported to undergo plug flow.[41,42] One requirement for plug flow is the rapid shear thinning of the hydrogel into a viscous fluid as demonstrated by our alginate hydrogels (Fig. 3D). We hypothesize that this plug flow behavior may be the mechanism by which cells are rescued from the damaging effects of extensional flow by alginate hydrogels. During plug flow, a portion of the hydrogel may retain its structural integrity and not become shear-thinned. Cells encapsulated within these hydrogel plugs may be shielded from deformation by extensional flow and shear by linear flow. Changing the alginate hydrogel formulation by altering the degree of crosslinking or the polymer molecular weight may impact the ability to undergo plug flow. This mechanical protection strategy relies only on the mechanical flow properties and is independent of cell properties. Therefore, this cell protection strategy should be broadly applicable to multiple cell types. Consistent with this idea, the alginate formulation that produced a hydrogel with $G' \sim 30$ Pa provided the most cell protection for all four cell types tested (Fig. 5).

In conclusion, stem cell transplantations are notoriously inefficient due to the low viability of transplanted cells. Currently, to overcome this low transplantation efficiency, a large quantity of cells must be transplanted to increase the likelihood of a successful procedure.[1,16] Our studies demonstrate a novel strategy to protect transplanted cells from the mechanical forces experienced during syringe needle flow that may reduce the stem cell concentration required for successful transplantation. Using fewer cells to achieve a similar number of transplanted, viable cells would greatly reduce the cost, time, and effort required for transplantation protocols.

Acknowledgments

B.A.A. was supported by a Stanford BioX Undergraduate Research Fellowship and a Stanford VPUE Major Grant. W.M. was supported by a Stanford BioX Graduate Research Fellowship. The authors acknowledge funding from the National Institutes of Health, 1DP2OD006477 and R01DK085720; the California Institute for Regenerative Medicine, RT2-01938; the Stanford Bio-X IIP4-22; and the National Science Foundation, EFRI-CBE-0735551. The authors thank Annelise Barron for rheometer use. Cells were kind gifts from Michael Longaker (hASC), Sanjiv Sam Gambhir (rMSC), and Theo Palmer (mNPC); Stanford Medical School.

Disclosure Statement

No competing financial interests exist.

References

1. Laflamme, M.A., Chen, K.Y., Naumova, A.V., Muskheli, V., Fugate, J.A., Dupras, S.K., Reinecke, H., Xu, C., Hassanipour, M., Police, S., O'Sullivan, C., Collins, L., Chen, Y., Minami, E., Gill, E.A., Ueno, S., Yuan, C., Gold, J., and Murry, C.E. Cardiomyocytes derived from human embryonic stem cells in pro-survival factors enhance function of infarcted rat hearts. Nat Biotechnol **25,** 1015, 2007.
2. Shapiro, A.M., Lakey, J.R., Ryan, E.A., Korbutt, G.S., Toth, E., Warnock, G.L., Kneteman, N.M., and Rajotte, R.V. Islet transplantation in seven patients with type 1 diabetes mellitus using a glucocorticoid-free immunosuppressive regimen. N Engl J Med **343,** 230, 2000.
3. Rafii, S., and Lyden, D. Therapeutic stem and progenitor cell transplantation for organ vascularization and regeneration. Nat Med **9,** 702, 2003.
4. Bliss, T., Guzman, R., Daadi, M., and Steinberg, G.K. Cell transplantation therapy for stroke. Stroke **38,** 817, 2007.
5. Willerth, S.M., and Sakiyama-Elbert, S.E. Cell therapy for spinal cord regeneration. Adv Drug Deliv Rev **60,** 263, 2008.
6. Nakagomi, N., Nakagomi, T., Kubo, S., Nakano-Doi, A., Saino, O., Takata, M., Yoshikawa, H., Stern, D.M., Mat-

suyama, T., and Taguchi, A. Endothelial cells support survival, proliferation, and neuronal differentiation of transplanted adult ischemia-induced neural stem/progenitor cells after cerebral infarction. Stem Cells **27,** 2185, 2009.
7. Tsur-Gang, O., Ruvinov, E., Landa, N., Holbova, R., Feinberg, M.S., Leor, J., and Cohen, S. The effects of peptide-based modification of alginate on left ventricular remodeling and function after myocardial infarction. Biomaterials **30,** 189, 2009.
8. Singelyn, J.M., DeQuach, J.A., Seif-Naraghi, S.B., Littlefield, R.B., Schup-Magoffin, P.J., and Christman, K.L. Naturally derived myocardial matrix as an injectable scaffold for cardiac tissue engineering. Biomaterials **30,** 5409, 2009.
9. Mazo, M., Planat-Benard, V., Abizanda, G., Pelacho, B., Leobon, B., Gavira, J.J., Penuelas, I., Cemborain, A., Penicaud, L., Laharrague, P., Joffre, C., Boisson, M., Ecay, M., Collantes, M., Barba, J., Casteilla, L., and Prosper, F. Transplantation of adipose derived stromal cells is associated with functional improvement in a rat model of chronic myocardial infarction. Eur J Heart Fail **10,** 454, 2008.
10. Wei, H., Ooi, T.H., Tan, G., Lim, S.Y., Qian, L., Wong, P., and Shim, W. Cell delivery and tracking in post-myocardial infarction cardiac stem cell therapy: an introduction for clinical researchers. Heart Fail Rev **15,** 1, 2010.
11. Tate, C.C., Shear, D.A., Tate, M.C., Archer, D.R., Stein, D.G., and LaPlaca, M.C. Laminin and fibronectin scaffolds enhance neural stem cell transplantation into the injured brain. J Tissue Eng Regen Med **3,** 208, 2009.
12. Cooke, M.J., Vulic, K., and Shoichet, M.S. Design of biomaterials to enhance stem cell survival when transplanted into the damaged central nervous system. Soft Matter **6,** 4988, 2010.
13. Kim, S.U., and de Vellis, J. Stem cell-based cell therapy in neurological diseases: a review. J Neurosci Res **87,** 2183, 2009.
14. Sortwell, C.E. Strategies for the augmentation of grafted dopamine neuron survival. Front Biosci **8,** s522, 2003.
15. Walsh, S., and Midha, R. Practical considerations concerning the use of stem cells for peripheral nerve repair. Neurosurg Focus **26,** E2, 2009.
16. Zhang, G., Hu, Q., Braunlin, E.A., Suggs, L.J., and Zhang, J. Enhancing efficacy of stem cell transplantation to the heart with a PEGylated fibrin biomatrix. Tissue Eng Part A **14,** 1025, 2008.
17. Bjorklund, A., Kirik, D., Rosenblad, C., Georgievska, B., Lundberg, C., and Mandel, R.J. Towards a neuroprotective gene therapy for Parkinson's disease: use of adenovirus, AAV and lentivirus vectors for gene transfer of GDNF to the nigrostriatal system in the rat Parkinson model. Brain Res **886,** 82, 2000.
18. Kordower, J.H., Freeman, T.B., Chen, E.Y., Mufson, E.J., Sanberg, P.R., Hauser, R.A., Snow, B., and Olanow, C.W. Fetal nigral grafts survive and mediate clinical benefit in a patient with Parkinson's disease. Mov Disord **13,** 383, 1998.
19. Zhang, M., Methot, D., Poppa, V., Fujio, Y., Walsh, K., and Murry, C.E. Cardiomyocyte grafting for cardiac repair: graft cell death and anti-death strategies. J Mol Cell Cardiol **33,** 907, 2001.
20. Cao, F., Sadrzadeh Rafie, A.H., Abilez, O.J., Wang, H., Blundo, J.T., Pruitt, B., Zarins, C., and Wu, J.C. *In vivo* imaging and evaluation of different biomatrices for improvement of stem cell survival. J Tissue Eng Regen Med **1,** 465, 2007.
21. Seif-Naraghi, S.B., Salvatore, M.A., Schup-Magoffin, P.J., Hu, D.P., and Christman, K.L. Design and characterization of an injectable pericardial matrix gel: a potentially autologous scaffold for cardiac tissue engineering. Tissue Eng Part A **16,** 2017, 2010.
22. Kong, H.J., Smith, M.K., and Mooney, D.J. Designing alginate hydrogels to maintain viability of immobilized cells. Biomaterials **24,** 4023, 2003.
23. Li, W., Ma, N., Ong, L.L., Nesselmann, C., Klopsch, C., Ladilov, Y., Furlani, D., Piechaczek, C., Moebius, J.M., Lutzow, K., Lendlein, A., Stamm, C., Li, R.K., and Steinhoff, G. Bcl-2 engineered MSCs inhibited apoptosis and improved heart function. Stem Cells **25,** 2118, 2007.
24. Bliss, T.M., Kelly, S., Shah, A.K., Foo, W.C., Kohli, P., Stokes, C., Sun, G.H., Ma, M., Masel, J., Kleppner, S.R., Schallert, T., Palmer, T., and Steinberg, G.K. Transplantation of hNT neurons into the ischemic cortex: cell survival and effect on sensorimotor behavior. J Neurosci Res **83,** 1004, 2006.
25. Uemura, M., Refaat, M.M., Shinoyama, M., Hayashi, H., Hashimoto, N., and Takahashi, J. Matrigel supports survival and neuronal differentiation of grafted embryonic stem cell-derived neural precursor cells. J Neurosci Res **88,** 542, 2010.
26. Rosso, F., Marino, G., Giordano, A., Barbarisi, M., Parmeggiani, D., and Barbarisi, A. Smart materials as scaffolds for tissue engineering. J Cell Physiol **203,** 465, 2005.
27. Zeng, Q., and Chen, W. The functional behavior of a macrophage/fibroblast co-culture model derived from normal and diabetic mice with a marine gelatin-oxidized alginate hydrogel. Biomaterials **31,** 5772, 2010.
28. Augst, A.D., Kong, H.J., and Mooney, D.J. Alginate hydrogels as biomaterials. Macromol Biosci **6,** 623, 2006.
29. Kuo, C.K., and Ma, P.X. Ionically crosslinked alginate hydrogels as scaffolds for tissue engineering: part 1. Structure, gelation rate and mechanical properties. Biomaterials **22,** 511, 2001.
30. Fang, Y., Al-Assaf, S., Phillips, G.O., Nishinari, K., Funami, T., Williams, P.A., and Li, L. Multiple steps and critical behaviors of the binding of calcium to alginate. J Phys Chem B **111,** 2456, 2007.
31. Becker, T.A., and Kipke, D.R. Flow properties of liquid calcium alginate polymer injected through medical microcatheters for endovascular embolization. J Biomed Mater Res **61,** 533, 2002.
32. Landa, N., Miller, L., Feinberg, M.S., Holbova, R., Shachar, M., Freeman, I., Cohen, S., and Leor, J. Effect of injectable alginate implant on cardiac remodeling and function after recent and old infarcts in rat. Circulation **117,** 1388, 2008.
33. Walker, P.A., Jimenez, F., Gerber, M.H., Aroom, K.R., Shah, S.K., Harting, M.T., Gill, B.S., Savitz, S.I., and Cox, C.S. Effect of needle diameter and flow rate on rat and human mesenchymal stromal cell characterization and viability. Tissue Eng Part C Methods **16,** 989, 2010.
34. Yu, J., Gu, Y., Du, K.T., Mihardja, S., Sievers, R.E., and Lee, R.J. The effect of injected RGD modified alginate on angiogenesis and left ventricular function in a chronic rat infarct model. Biomaterials **30,** 751, 2009.
35. Park, H., Kang, S.W., Kim, B.S., Mooney, D.J., and Lee, K.Y. Shear-reversibly crosslinked alginate hydrogels for tissue engineering. Macromol Biosci **9,** 895, 2009.
36. Pinto, R., Medronho, R., and Castilho, L. Separation of CHO cells using hydrocyclones. Cytotechnology **56,** 57, 2008.
37. Lee, S.S., Yim, Y., Ahn, K.H., and Lee, S.J. Extensional flow-based assessment of red blood cell deformability using hyperbolic converging microchannel. Biomed Microdevices **11,** 1021, 2009.
38. Tanzeglock, T., Soos, M., Stephanopoulos, G., and Morbidelli, M. Induction of mammalian cell death by simple shear and extensional flows. Biotechnol Bioeng **104,** 360, 2009.

39. Schroeder, C.M., Babcock, H.P., Shaqfeh, E.S., and Chu, S. Observation of polymer conformation hysteresis in extensional flow. Science **301,** 1515, 2003.
40. Maroja, A.M., Oliveira, F.A., Michal, M., and Longa, L. Polymer fragmentation in extensional flow. Phys Rev E Stat Nonlin Soft Matter Phys **63,** 061801, 2001.
41. Olsen, B.D., Kornfield, J.A., and Tirrell, D.A. Yielding behavior in injectable hydrogels from telechelic proteins. Macromolecules **43,** 9094, 2010.
42. Yan, C., Altunbas, A., Yucel, T., Nagarkar, R.P., Schneider, J.P., and Pochan, D.J. Injectable solide hydrogel: mechanism of shear-thinning and immediate recovery of injectable β-hairpin peptide hydrogels. Soft Matter **6,** 5143, 2010.

Address correspondence to:
Sarah C. Heilshorn, Ph.D.
Department of Materials Science and Engineering
Stanford University
476 Lomita Mall
McCullough Room 246
Stanford, CA 94305-4045

E-mail: heilshorn@stanford.edu

Received: July 11, 2011
Accepted: October 18, 2011
Online Publication Date: December 19, 2011